Article

Corresponding Author:

Houman Rokni, Afton Chemical Ltd., Bracknell, Berkshire, RG12 2UW, UK & Department of Mechanical Engineering and Aeronautics, City University of London, Northampton Square, EC1V 0HB London, UK

Email: houman.rokni@aftonchemical.com

Entropy scaling based viscosity predictions for hydrocarbon mixtures and diesel fuels up to extreme conditions

Houman B. Rokni [1, 2], Joshua D. Moore[3], Ashutosh Gupta[3], Mark A. McHugh[4], and Manolis Gavaises[2]

[1]Afton Chemical Ltd., Bracknell, Berkshire, RG12 2UW, UK
[2]Department of Mechanical Engineering and Aeronautics, City, University of London, Northampton Square, EC1V 0HB London, UK
[3]Afton Chemical Corp., Richmond, Virginia 23219, USA
[4]Department of Chemical and Life Science Engineering, Virginia Commonwealth University, Richmond, Virginia 23284, USA

Abstract

An entropy scaling based technique using the Perturbed-Chain Statistical Associating Fluid Theory is described for predicting the viscosity of hydrocarbon mixtures and diesel fuels up to high temperatures and high pressures. The compounds found in diesel fuels or hydrocarbon mixtures are represented as a single pseudo-component. The model is not fit to viscosity data but is predictive up to high temperatures and pressures with input of only two calculated or measured mixture properties: the number averaged molecular weight and hydrogen to carbon ratio. Viscosity is predicted less accurately when the mixture contains high concentrations of iso-alkanes and cyclohexanes. However, it is shown that predictions for these mixtures are improved by fitting a

third parameter to a single viscosity data point at a chosen reference state. For hydrocarbon mixtures, viscosity is predicted with average mean absolute percent deviations (MAPDs) of 12.2% using the two-parameter model and 7.3% using the three-parameter model from 293 to 353 K and up to 1,000 bar. For two different diesel fuels, viscosity is predicted with an average MAPD of 21.4% using the two-parameter model and 9.4% using the three-parameter model from 323 to 423 K and up to 3,500 bar.

Introduction

Fuel injectors are key systems that determine the performance, emissions, and fuel economy of diesel engines [1, 2]. Operation and performance of fuel injectors are sensitive to fluid properties, including density, viscosity, and volatility. Emission regulations and the need for improved fuel economy have motivated diesel engine manufacturers to increase fuel injector operating pressures up to 4,500 bar [3]. Furthermore, fuel injectors need to perform across a range of commercially available diesel fuels, whose composition and fluid properties vary in different markets. Experimental development, testing, and validation of these technologies is a significant time and resource-intensive process.

Computational fluid dynamics (CFD) simulations are used to model the performance of fuel injectors and to investigate phenomena such as cavitation and fuel atomization [4-10]. The accuracy of CFD simulation up to extreme pressures depends on accurate representation of fuel thermophysical properties (*e.g.*, viscosity, density, heat capacity, and thermal conductivity) as a function of temperature and pressure. For example, Theodorakakos et al. [11] calculated that mass flow was overestimated by 7% if the temperature and pressure dependence of thermophysical properties was not included in CFD models of diesel fuel injectors.

Temperature and pressure dependence of thermophysical properties can be incorporated in CFD through empirical correlations, look-up tables, or equations of state (EoS). These approaches most often require fitting or measurement of experimental data, which is rarely available for diesel fuels up to high temperatures and high pressures (HTHP). At high pressures, compositional variance between fuels can lead to significant differences in viscosity. For example, the viscosity of two different diesel fuels reported by Aquing et al. [13] and Schaschke et al. [12] at 323 K differ by more than 120% at 1,800 bar and 200% at 2,400 bar. Models fit to viscosity data for one diesel sample cannot be expected to accurately represent the viscosity of another diesel of different composition. Therefore, predictive viscosity models are needed that account for temperature, pressure, and composition. Ideally, the models should require minimal input of HTHP experimental data to reduce characterization expense.

Several correlations and theories have been proposed to model the viscosity of pure components and mixtures as a function of temperature and pressure [14]. These include empirical models and correlations and pseudo-component approaches. Empirical models and correlations [15-21] have been used to predict the viscosity of complex mixtures (*e.g.*, crude oils, bitumens, heavy oils, and diesel and biodiesel fuels) and their blends.

Recently, several researchers demonstrated advantages when incorporating advanced equations of state (EoS), such as the Perturbed-Chain Statistical Associating Fluid Theory (PC-SAFT) within CFD [22-24]. Given that complex mixtures (*e.g.*, diesel and biodiesel fuels, crude oils, bitumens, heavy oils) are often composed of hundreds of different compounds [13, 25-29], CFD simulation of every fuel compound would be computationally intensive. Often, a smaller number of components are chosen as a surrogate to closely match the thermophysical properties of the mixture [13, 30-36]. Selection of the individual components and their concentrations is challenging, and a

surrogate of one fuel may not accurately represent the properties of another fuel with a different composition.

Computational cost and complexity can be reduced further through pseudo-component viscosity mixture models. Examples of these models include expanded fluid theory (EFT) [37-40], friction theory (FT) [41-45], free volume theory (FVT) [46, 47], the Dymond-Assael (DA) hard sphere model [48-50], and Eyring's absolute rate theory [51, 52]. Motahhari et al. [38, 39] applied EFT to model the viscosity of several crude oils characterized as mixtures of pseudo-components at temperatures to 473 K and pressures to 552 bar. They fit EFT parameters to atmospheric viscosity data for some crude oils and predicted the parameters for others. Ma et al. [40] used EFT to predict the viscosity of two bitumens characterized with a single pseudo-component at temperatures to 463 K and pressures to 100 bar.

Schmidt et al. [44] applied FT to model the viscosity of a North Sea crude oil represented as a mixture of pseudo-components to temperatures of 375 K and pressures to approximately 500 bar. They obtained the values for the FT parameters by fitting individual isotherms for pressures to approximately 350 bar. In a different study, Quiñones-Cisneros et al. [42, 43] applied FT to model the viscosity of crude oils represented as mixtures of pseudo-components to pressures up to 400 bar. These authors fit FT parameters to viscosity data above the saturation pressure and made predictions below the saturation pressure. Abutaqiya et al. [45] applied FT to model the viscosity of ten Middle Eastern crude oils represented as mixtures of pseudo-components. These authors proposed a new fitting approach for FT and reduced the required number of input parameters for each pseudo-component from two to one. The fitted parameter was adjusted to a single data point at saturation, and viscosities were predicted for temperatures to 400 K and pressures to 600 bar.

Using FVT, Khoshnamvand and Assareh [46] modeled the viscosity of live oils. Their model defined mixtures containing multiple components including a pseudo-component representing C7+ (*i.e.*, compounds with carbon numbers (CNs) greater than 6). They fit FVT parameters to experimental data for 22 live oils as a training set, and they predicted viscosity of six other oils.

Ijaz [50] predicted the viscosity of crude oils through single pseudo-components using the DA hard sphere model [48, 49]. Ijaz fit four parameters in the model to experimental data and predicted the viscosity of crude oils up to 448 K and 1,400 bar. In a different approach, Macias-Salinas et al. [51] represented several crude oils through mixtures of pseudo-components and modeled the mixture viscosity using Eyring's absolute rate theory [52]. They used a tuning factor to scale density and viscosity predictions, which required fitting the model to experimental data.

Entropy scaling is another approach reported for modeling viscosity. First proposed by Rosenfeld [53], entropy scaling effectively reduces the temperature and pressure dependence of viscosity to a mono-variable dependence on residual entropy. Recently, Lötgering-Lin and Gross utilized Rosenfeld's entropy scaling approach to develop a group contribution (GC) method using PC-SAFT to predict the viscosity of pure components [54] and mixtures [55]. Fouad and Vega [56, 57] also used entropy scaling to model the viscosity of hydroflurocarbon and hydrofluroolefin refrigerants, fitting parameters to experimental saturated viscosity data.

The present study describes an entropy scaling based single pseudo-component technique using the PC-SAFT EoS [54] to predict the viscosity of hydrocarbon mixtures and diesel fuels. The pseudo-component technique [58] is applied to correlate reduced viscosity to residual entropy through a third order polynomial using the GC method of Lötgering-Lin and Gross [54]. The model is not fit to viscosity data but is predictive up to HTHP conditions using two calculated or measured mixture properties: the number averaged molecular weight (MW) and hydrogen to carbon (HN/CN)

ratio. Deviations in predictions are found when the mixture contains large concentrations of iso-alkanes and cyclohexanes. However, this deviation is reduced when a third mixture property, viscosity at a chosen reference state, is used to fix the value of one of the model parameters. Pseudo-component viscosity predictions are compared to experimental data for 54 different hydrocarbon mixture compositions and two diesel fuels over a wide range of temperatures and pressures.

Technique Development

PC-SAFT pseudo-component technique

The pseudo-component technique is developed using the PC-SAFT EoS of Gross and Sadowski [59] combined with the GC residual entropy method of Lötgering-Lin and Gross [54] to predict the viscosity of hydrocarbon mixtures and diesel fuels. The compounds in these mixtures do not exhibit complex formation or association, such as hydrogen bonding. Hence, the PC-SAFT EoS only requires three parameters: m, the number of segments; σ, the segment diameter; and ε/k, the depth of the potential well. The reduced, residual Helmholtz free energy, $\tilde{a}^{\mathrm{res}}$, of a pure component is then expressed as:

$$\tilde{a}^{\mathrm{res}} = \tilde{a}^{\mathrm{hc}} + \tilde{a}^{\mathrm{disp}} \tag{1}$$

where $\tilde{a}^{\mathrm{hc}}$ and $\tilde{a}^{\mathrm{disp}}$ are the reduced, Helmholtz free energies for the hard-chain reference fluid and dispersion interactions, respectively.

Here we briefly describe how to calculate the pseudo-component parameters needed with the PC-SAFT EoS; details can be found elsewhere [58]. The GC method of Sauer et al. [60] is used to generate the correlations shown in Table 1 for n-alkanes and PNAs that provide the numerical bounds for the pseudo-component m, σ, and ε/k values. These numerical bounds encompass the

PC-SAFT parameters for all of the other chemical compounds found in a typical fuel. Equations 2 to 4 show how the pseudo-component parameters are weighted with the parameter Z, which varies from zero for n-alkanes to 1.0 for PNAs [58]. Equation 5 is used to calculate Z knowing the mixture degree of unsaturation (DoU) and the mixture number averaged MW and HN/CN ratio (Eqs. 6 and 7). If all of the mixture components are known, the HN/CN ratio can be directly calculated; otherwise this ratio can be measured with elemental analysis, which is the typical approach used with complex fuel mixtures, such as diesel. The Supplemental Information (SI) provides the DoU correlation for PNAs as a function of MW. However, here we note that phenanthrene (MW = 178 g/mol, DoU = 10) is the largest PNA in the hydrocarbon mixtures and diesel fuels considered in this study. Hence, $\mathrm{DoU_{PNA}}$ is fixed with an upper bound of 10 in Eq. 5 when the mixture number averaged MW is greater than 178 g/mol so as not to over predict the n-alkane contribution to the pseudo-component parameters. Equation 8 can now be used with the PC-SAFT EoS to calculate the reduced residual entropy, $\tilde{s}^{\mathrm{res}}$ (*i.e.*, the molar residual entropy, $\bar{s}^{\mathrm{res}}$, divided by the gas constant, *R*), using commercial software (VLXE/Blend [61]). The next section describes the steps needed for the calculation of the viscosity knowing $\tilde{s}^{\mathrm{res}}$.

Table 1. PC-SAFT parameter correlations as a function of MW (g/mol) for n-alkanes and PNAs using the GC parameters of Sauer et al. [60].

	n-alkane	PNA
m	$0.0325\mathrm{MW} + 0.2463$	$0.0231\mathrm{MW} + 0.7392$
$m\sigma$ (Å)	$0.1265\mathrm{MW} + 0.7564$	$0.0874\mathrm{MW} + 2.6366$
ε/k (K)	$\exp(5.4762 - 1.3302/\mathrm{MW})$	$\exp(5.8137 - 15.5549/\mathrm{MW})$

$$m_{\text{pseudo}-\text{component}} = (1-Z)m_{\text{n}-\text{alkane}} + Zm_{\text{PNA}} \tag{2}$$

$$(m\sigma)_{\text{pseudo}-\text{component}} = (1-Z)(m\sigma)_{\text{n}-\text{alkane}} + Z(m\sigma)_{\text{PNA}} \tag{3}$$

$$\left(\varepsilon/k\right)_{\text{pseudo}-\text{component}} = (1-Z)\left(\varepsilon/k\right)_{\text{n}-\text{alkane}} + Z\left(\varepsilon/k\right)_{\text{PNA}} \tag{4}$$

$$Z = \begin{cases} \dfrac{\text{DoU}_{\text{mixture}}}{\text{DoU}_{\text{PNA}}}, & \text{MW}_{\text{mixture}} < 178\ \text{g/mol} \\ \dfrac{\text{DoU}_{\text{mixture}}}{10}, & \text{MW}_{\text{mixture}} \geq 178\ \text{g/mol} \end{cases} \tag{5}$$

$$\text{CN} = \frac{\text{MW}_{\text{mixture}}}{12.01 + 1.01(\text{HN}/\text{CN})} \tag{6}$$

$$\text{DoU} = \frac{1}{2}(2 \times \text{CN} + 2 - \text{HN}) \tag{7}$$

$$\tilde{s}^{\text{res}}(V,T) = -\left(\frac{\partial \tilde{a}^{\text{res}}}{\partial T}\right)_V \tag{8}$$

Entropy scaling based pseudo-component technique

Rosenfeld [53] showed that the reduced viscosity, $\eta^* = \eta/\eta_{\text{reference}}$, scales with $\tilde{s}^{\text{res}}$. Here $\eta_{\text{reference}}$ is set equal to the Chapman-Enskog viscosity (Eq. 9), as recommended by Novak [62, 63] who showed that a straightforward scaling of $\tilde{s}^{\text{res}}$, over the entire fluid phase space, can be obtained.

$$\eta_{\text{reference}} = \frac{5}{16}\frac{\sqrt{MWk\,T/(mN_{\text{A}}\pi)}}{\sigma^2\Omega(2,2)^*} \tag{9}$$

where m and σ are the PC-SAFT parameters for a pure compound when calculating viscosity for a pure compound or are those of a pseudo-component when calculating viscosity of a pseudo-component. In Eq. 9, T, k, N_{A}, and $\Omega^{(2,2)*}$ are temperature, Boltzmann's constant, Avogadro's number, and the reduced collision integral, respectively. The correlation of Neufeld et al. [64] is used to calculate $\Omega^{(2,2)*}$. Lötgering-Lin and Gross [54] modified Novak's approach to calculate η^* by using a third-order polynomial (Eq. 10) in reduced dimensionless residual entropy, s^* (Eq. 11). propose

$$ln(\eta^*) = A + Bs^* + Cs^{*2} + Ds^{*3} \tag{10}$$

$$s^* = \left(\frac{\tilde{s}^{\mathrm{res}}(V,T)}{m}\right) \tag{11}$$

In Eq. 10, A, B, C, and D are the viscosity coefficients of either a pure compound or pseudo-component needed to calculate the viscosity. For a pure compound, these viscosity coefficients are found to best correlate to MW when each coefficient is multiplied by m^2. As a typical result, Figure 1 shows the variation of Am^2 with MW for selected compounds found in diesel fuels, where A is calculated using the GC method of Lötgering-Lin and Gross [54] and $m = m_{\text{pure compound}}$. The Am^2 values that fall outside the alkane and PNA curves are ignored since these compounds have MWs less than those of the diesels considered in this study [58]. Figure 2 shows the variation of Am^2, Bm^2, Cm^2, and Dm^2 with MW for n-alkanes and PNAs and Table 2 lists the coefficients for the polynomial fits needed to calculate each viscosity coefficient. The previously determined Z parameter is now used in Eqs. 12-15 to calculate the pseudo-component viscosity coefficients needed in Eq. 10.

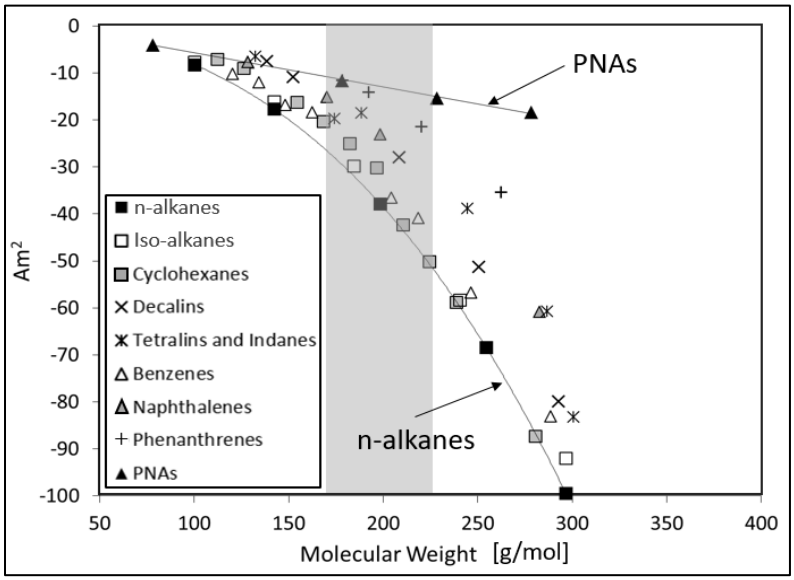

Figure 1. Effect of molecular weight on Am^2 for selected compounds with A calculated using the GC method of Lötgering-Lin and Gross [54] and with $m = m_{\text{pure compound}}$. The shaded region shows the number averaged MW range (*i.e.*, 172 to 228 g/mol) for the diesel fuels studied by Aquing et al. [13].

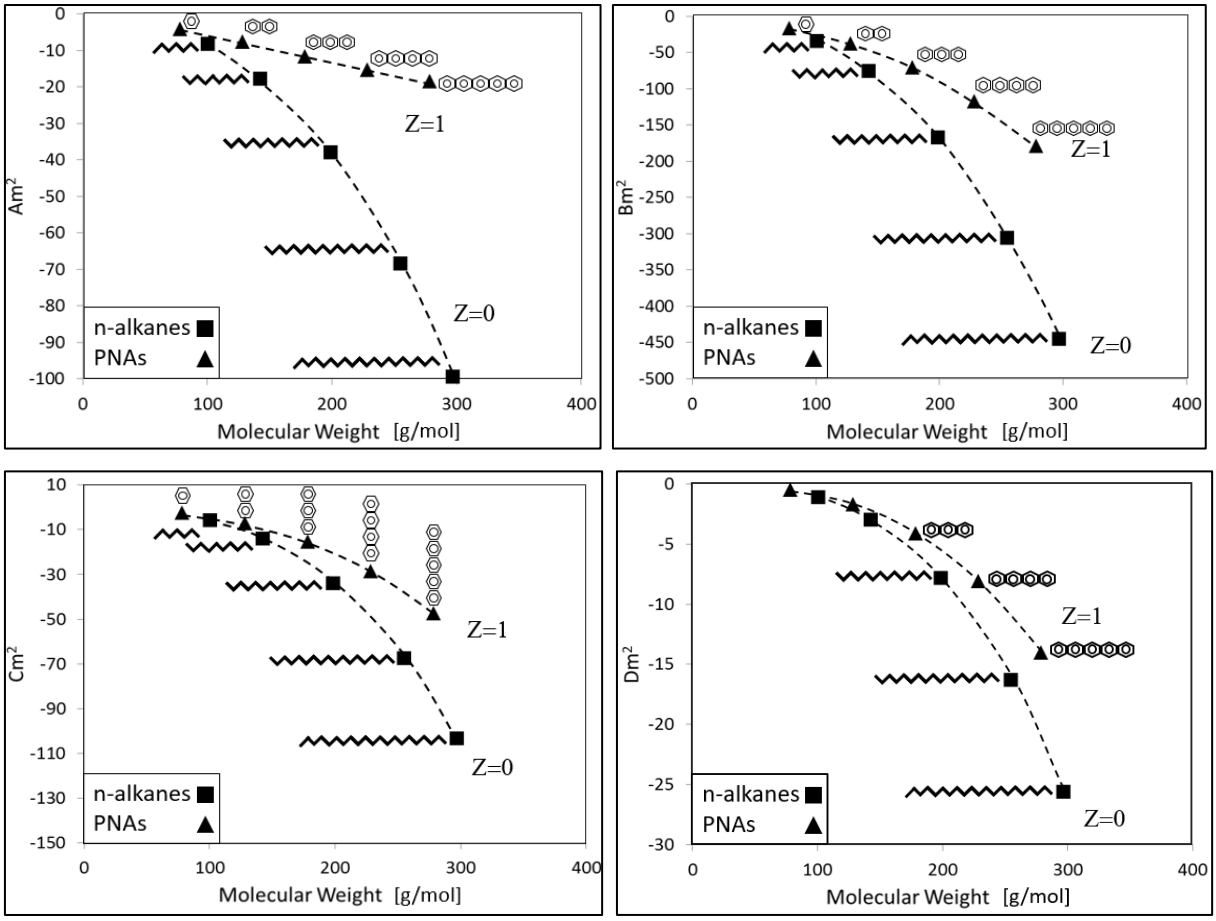

Figure 2. Effect of molecular weight on the viscosity coefficients for n-alkanes and PNAs calculated using the GC method of Lötgering-Lin and Gross [54] and with $m = m_{\text{pure compound}}$. Structures of representative compounds are shown in the figures.

Table 2. Parameters for the 3rd order polynomial correlation as a function of MW (g/mol) for the viscosity coefficients of n-alkanes and PNAs: $Ym^2 = \sum_{i=0}^{3}\left(e_i MW^i\right)$. Y is a viscosity coefficient (A, B, C or D) and e is the coefficient in the polynomial equation for n-alkanes and PNAs.

	n-alkane				PNA			
	e_0	e_1	e_2	e_3	e_0	e_1	e_2	e_3
Am^2	-3.000×10^{-2}	-8.028×10^{-3}	-5.510×10^{-4}	-1.860×10^{-6}	-3.996×10^{-1}	-2.420×10^{-2}	-3.431×10^{-4}	7.111×10^{-7}
Bm^2	-1.602×10^{1}	3.079×10^{-1}	-4.279×10^{-3}	-5.524×10^{-6}	-2.194×10^{0}	-4.339×10^{-2}	-1.522×10^{-3}	-2.172×10^{-6}
Cm^2	-9.298×10^{-3}	-2.639×10^{-3}	-2.107×10^{-4}	-3.215×10^{-6}	-1.020×10^{-1}	-7.812×10^{-3}	-1.895×10^{-4}	-1.408×10^{-6}
Dm^2	1.085×10^{-4}	-2.519×10^{-5}	-1.232×10^{-5}	-9.383×10^{-7}	1.644×10^{-3}	-4.411×10^{-4}	-3.231×10^{-5}	-5.288×10^{-7}

$$\left(Am^2\right)_{\text{pseudo}-\text{component}} = (1-Z)\left(Am^2\right)_{\text{n}-\text{alkane}} + Z\left(Am^2\right)_{\text{PNA}} \quad (12)$$

$$\left(Bm^2\right)_{\text{pseudo}-\text{component}} = (1-Z)\left(Bm^2\right)_{\text{n}-\text{alkane}} + Z\left(Bm^2\right)_{\text{PNA}} \quad (13)$$

$$\left(Cm^2\right)_{\text{pseudo}-\text{component}} = (1-Z)\left(Cm^2\right)_{\text{n}-\text{alkane}} + Z\left(Cm^2\right)_{\text{PNA}} \quad (14)$$

$$\left(Dm^2\right)_{\text{pseudo}-\text{component}} = (1-Z)\left(Dm^2\right)_{\text{n}-\text{alkane}} + Z\left(Dm^2\right)_{\text{PNA}} \quad (15)$$

It should be noted that improved predictions can be obtained in some cases if *D* is fit to a single viscosity data point rather than calculating *D* with Eq. 15. Both approaches shown in the following section require information on the mixture number averaged MW and HN/CN ratio. For convenience, *D* is fit to a viscosity experimental data point at the lowest reported temperature and

pressure (*e.g.,* 323 K and ~10 bar for the two diesel fuels in this study). An equally appropriate approach is to fit D to the kinematic viscosity at 40 °C (KV40 [65]) or to the viscosity at atmospheric pressure and room temperature since both types of data are commonly measured in industry.

Viscosity predictions are compared with 1822 literature data points for the hydrocarbon mixtures and diesel fuels. For mixtures where experimental data for more than three isotherms are available, only the lowest, a central, and the highest temperature isotherms are shown for clarity. However, all available experimental data are included in the calculation of the maximum (Max) deviation, standard deviation (SD), MAPD, and bias in Eqs. 16-20.

$$\text{Deviation (\%)} = 100 \times \frac{\left(\eta_{\text{predict}} - \eta_{\text{exp}}\right)}{\eta_{\text{exp}}} \tag{16}$$

$$\text{Max Deviation (\%)} = Max\left(100 \times \frac{\left|\eta_{\text{predict}} - \eta_{\text{exp}}\right|}{\eta_{\text{exp}}}\right) \tag{17}$$

$$\text{SD (\%)} = \sqrt{\frac{\sum(\eta - \bar{\eta})^2}{N-1}} \tag{18}$$

$$\text{MAPD (\%)} = \frac{1}{N}\sum 100 \times \frac{\left|\eta_{\text{predict}} - \eta_{\text{exp}}\right|}{\eta_{\text{exp}}} \tag{19}$$

$$\text{Bias (\%)} = \frac{1}{N}\sum 100 \times \frac{\left(\eta_{\text{predict}} - \eta_{\text{exp}}\right)}{\eta_{\text{exp}}} \tag{20}$$

where η_{exp}, η_{predict}, N, and $\bar{\eta}$ are the experimental viscosity data point, the predicted viscosity, the number of data points, and the viscosity mean, respectively.

Hydrocarbon Mixtures

Table 3 lists the molar compositions of hydrocarbon mixtures used to evaluate the viscosity pseudo-component technique. Zeberg-Mikkelsen et al. [66] measured the viscosity of ternary mixtures (referred to as M1) containing methyl-cyclohexane (MCH), decalin, and 2,2,4,4,6,8,8-heptamethyl-nonane (*i.e.*, iso-cetane) for three different compositions at seven temperatures (293, 303, 313, 323, 343, and 353 K) and pressures up to 1,000 bar. Baylaucq et al. [67] reported the viscosity for ternary mixtures (referred to as M2) containing n-heptane (C7), MCH, and methyl-naphthalene for twenty-one compositions at three temperatures (303, 323, and 343 K) and pressures up to 1,000 bar. Boned et al. [68] reported viscosity measurements for a ternary (referred to as M3) and a quinary (referred to as M4) mixture at seven temperatures (293, 303, 313, 323, 333, 343, and 353 K) and pressures up to 1,000 bar. Dauge et al. [69] measured the viscosity of binary mixtures (referred to as M5) containing iso-cetane and normal-tridecane (C13) for seven compositions at seven temperatures (293, 303, 313, 323, 333, 343, and 353 K) and pressures up to 1,000 bar. Zeberg-Mikkelsen et al. [70] reported the viscosity for ternary mixtures (referred to as M6) containing iso-cetane, C13, and methyl-naphthalene for twenty-one compositions at seven temperatures (293, 303, 313, 323, 333, 343, and 353 K) and pressures up to 1,000 bar.

Table 3. Molar composition of the mixtures studied in this work [66-70] and viscosity of compounds present in these mixtures at 298 K and 1 atmosphere [71-79].

Compound	Chemical Family	Viscosity (cP)	M1	M2	M3	M4	M5	M6
n-heptane	n-alkanes	0.388	-	0.125-0.750	-	-	-	-
n-tridecane	n-alkanes	2.130	-	-	0.394	0.200	0.125-0.875	0.125-0.750
2,2,4,4,6,8,8-heptamethyl-nonane	Iso-alkanes	3.354	balance	-	-	0.162	balance	0.125-0.750
methyl-cyclohexane	Cyclohexanes	0.681	0.125-0.333	0.125-0.750	-	-	-	-
heptyl-cyclohexane	Cyclohexanes	2.473	-	-	0.348	0.353	-	-
decalin	Decalins	2.469	0.125-0.333	-	-	-	-	-
heptyl-benzene	Benzenes	2.100	-	-	0.258	0.156	-	-
methyl-naphthalene	Naphthalenes	2.913	-	balance	-	0.129	-	balance

Figures 3 and 4 show the viscosity predictions and deviations from experiment, respectively, for the hydrocarbon mixtures reported by Zeberg-Mikkelsen et al. [66], Baylaucq et al. [67], Boned et al. [68], Dauge et al. [69], and Zeberg-Mikkelsen et al. [70]. For brevity, only central compositions are included in the figures. For mixture viscosities measured by Zeberg-Mikkelsen et al. [66], only the data for mixture composition containing 0.250 mole fraction MCH, 0.250 mole fraction decalin, and 0.500 mole fraction iso-octane (referred to as M1-2) are shown in the figures. For mixture viscosities measured by Baylaucq et al. [67], only the data for mixture composition containing 0.250 mole fraction C7, 0.625 mole fraction MCH, and 0.125 mole fraction of methyl-naphthalene (referred to as M2-11) are shown in the figures. For mixture viscosities measured by Dauge et al. [69], only the data for mixture composition containing 0.500 mole fraction C13 and 0.500 mole fraction of iso-cetane (referred to as M5-4) are shown in the figures. For mixture viscosities measured by Zeberg-Mikkelsen et al. [70], only the data for mixture composition containing 0.125

mole fraction iso-cetane, 0.625 mole fraction C13, and 0.250 mole fraction of methyl-naphthalene (referred to as M6-11) are shown in the figures. Table 4 lists the calculated MW, HN/CN ratio, Z parameter, viscosity experimental data point (η_o) at the lowest reported temperature and pressure used to fit D in the three parameter model, the PC-SAFT parameters, and the viscosity coefficients for the pseudo-components for the hydrocarbon mixtures shown in the figures. Table 5 summarizes viscosity predictions of the hydrocarbon mixtures. Parameters and MAPDs are reported in the SI for all hydrocarbon mixture compositions in this study.

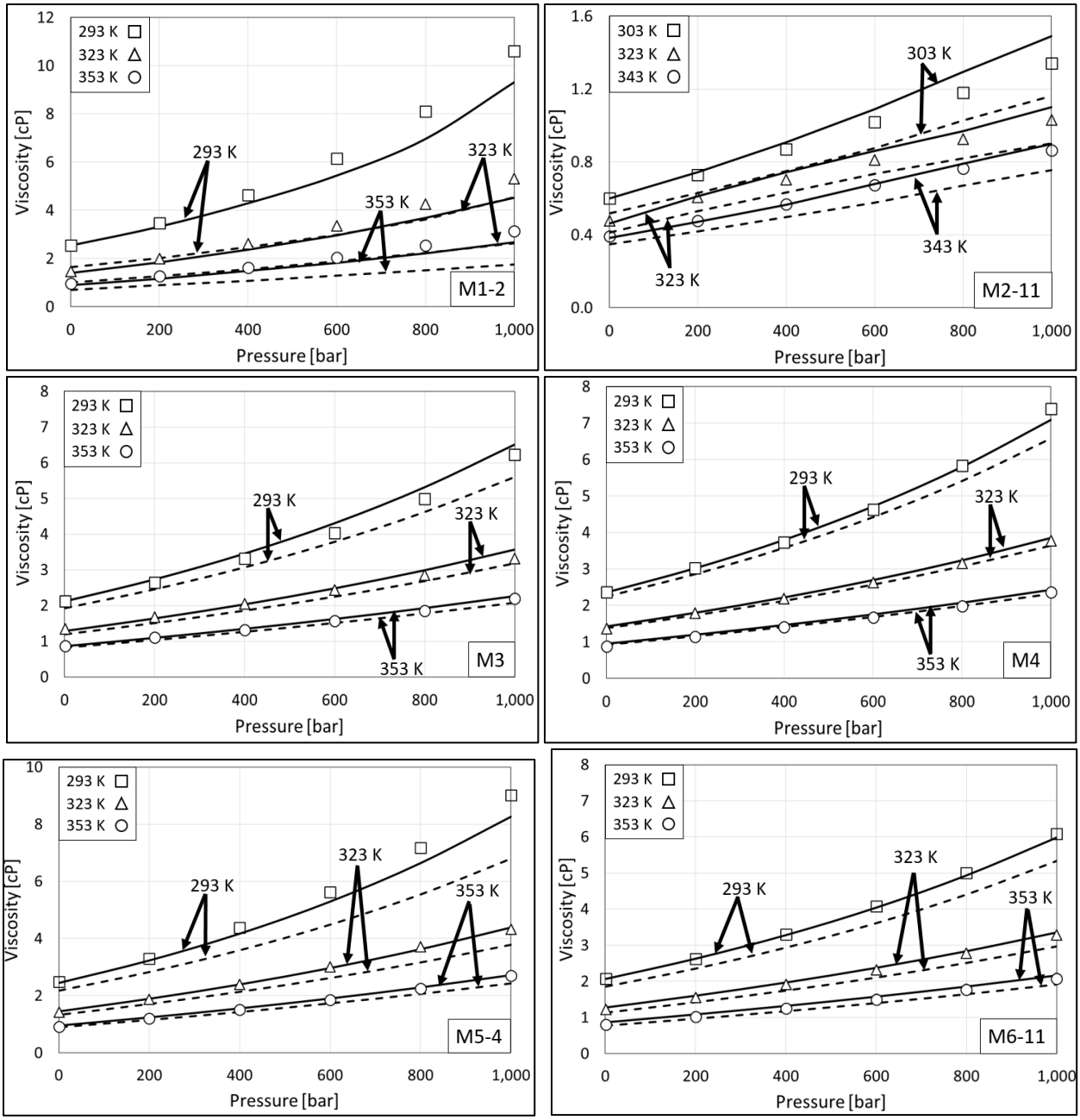

Figure 3. Pseudo-component viscosity predictions compared to experimental data [66-70] (symbols) for hydrocarbon mixtures listed in Table 3: two-parameter (dashed lines) and three-parameter (solid lines) models. Note that the y-axis scale is different in each figure.

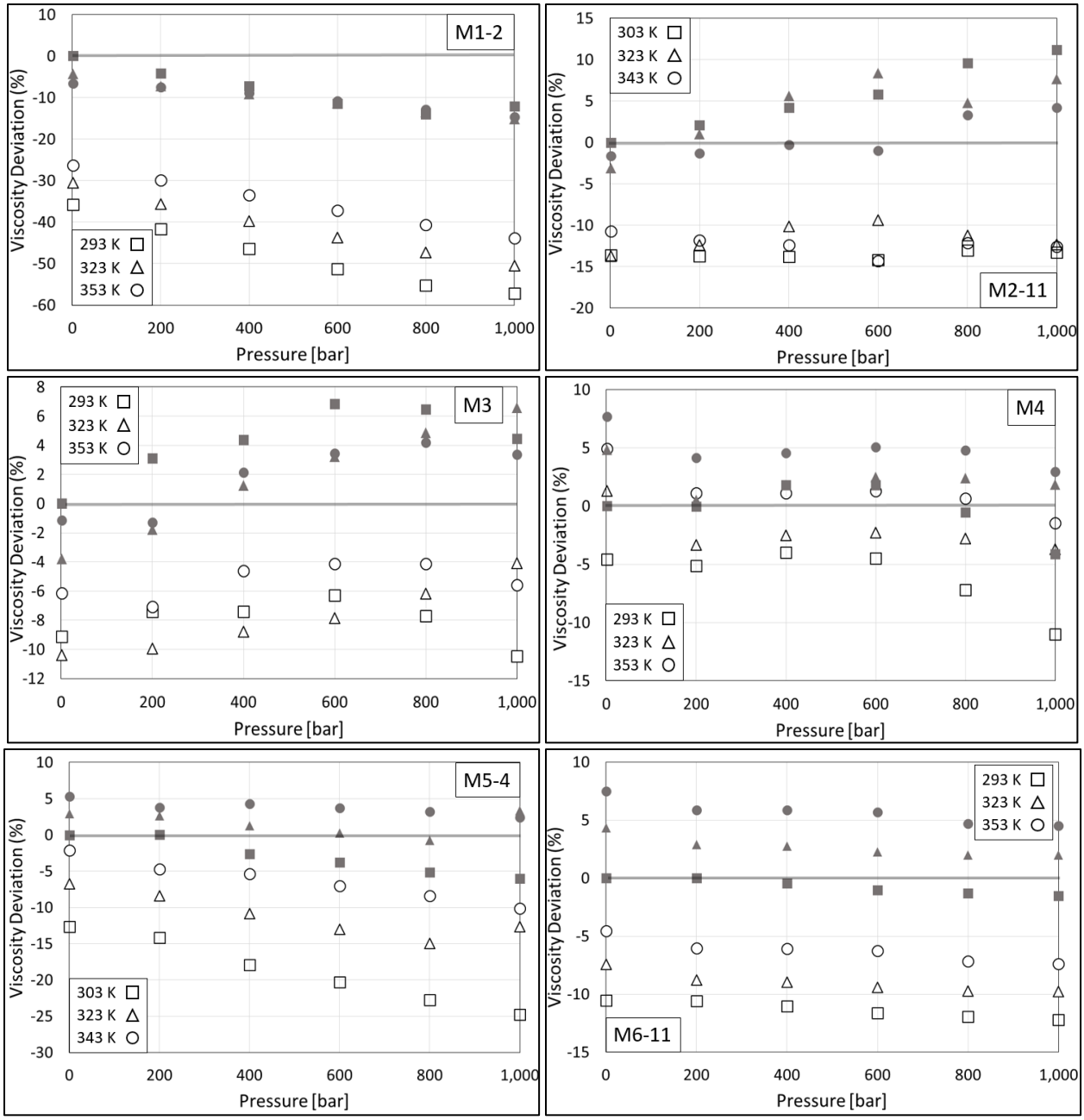

Figure 4. Pseudo-component viscosity deviations compared to experimental data [66-70] for hydrocarbon mixtures listed in Table 3: two-parameter (open symbols) and three-parameter (filled symbols) models. Note that the y-axis scale is different in each figure.

Table 4. Pseudo-component properties and parameters for mixtures shown in Figure 3. η_o is the viscosity data point at the lowest reported temperature and pressure (1 bar) used to fit D, now termed D^{fit}, in the three-parameter model.

Mixture	MW	HN/CN	Z	η_o / cP	m	σ (Å)	ε/k (K)	A	B	C	D	D^{fit}
M1-2	172.3	2.01	0.097	2.54 at 293 K	5.736	3.849	244.5	-0.781	-3.439	-0.678	-0.153	-0.199
M2-11	104.2	1.94	0.220	0.60 at 303 K	3.526	3.816	248.0	-0.665	-2.754	-0.470	-0.093	-0.111
M3	181.6	1.94	0.139	2.12 at 293 K	5.980	3.847	247.6	-0.788	-3.519	-0.706	-0.162	-0.172
M4	183.8	1.84	0.206	2.36 at 293 K	5.965	3.841	252.2	-0.776	-3.520	-0.712	-0.165	-0.169
M5-4	205.4	2.14	0	2.49 at 293 K	6.922	3.863	237.4	-0.857	-3.511	-0.779	-0.181	-0.196
M6-11	179.1	1.84	0.204	2.07 at 293 K	5.824	3.840	251.4	-0.770	-3.476	-0.698	-0.161	-0.158

Table 5. The MAPD (%), bias (%), SD (%), and Max Deviation (%) for pseudo-component viscosity predictions of hydrocarbon mixtures compared to the literature data [66-70].

	Two-parameter						Three-parameter					
	M1	M2	M3	M4	M5	M6	M1	M2	M3	M4	M5	M6
MAPD	35.0	8.0	7.2	3.1	14.0	10.2	11.0	4.8	3.4	2.8	4.6	5.2
Bias	-35.0	-4.8	-7.2	-2.1	-14.0	-7.9	-10.9	3.5	2.1	2.5	-0.3	-2.2
SD	10.1	5.1	2.1	2.1	8.8	7.5	7.3	4.2	2.1	1.9	4.2	4.7
Max Deviation	56.7	24.4	11.6	11.0	49.0	38.7	26.7	24.6	7.8	7.7	22.9	25.5

Viscosities are predicted for mixtures M1 and M2 with average MAPDs of 35 and 8%, respectively when using the two-parameter model. Although the average MAPD for viscosity

predictions for compositions of mixture M2 is less than for compositions of mixture M1, the MAPDs for both mixtures are shown in the SI to increase with MCH concentration. When using the two-parameter model, viscosities are predicted for mixture M1-3 (33.3 mol% MCH) and mixture M2-6 (75.0 mol% MCH) with 45 and 20% MAPDs, respectively. More accurate viscosities are predicted using the two-parameter model for mixtures M3 and M4 (7.2 and 3.1% MAPD, respectively), which do not contain MCH. Viscosities of mixtures M5 and M6, which contain large concentrations of iso-cetane, are predicted with average MAPDs of 14 and 10%, respectively using the two-parameter model. Due to the definition of DoU (Eq. 7), the pseudo-component technique does not distinguish normal and iso-alkanes, which could be a reason for viscosity prediction deviations, when significant concentrations of iso-alkanes are present in the mixtures. Predictions for all hydrocarbon mixtures in this study are improved by fitting the *D* coefficient (three-parameter model).

It should be noted that MCH (MW = 98.18 g/mol) lies at the extreme lower bounds of the fitted PC-SAFT and viscosity coefficient correlations, where the n-alkane and PNA correlations converge to the approximately the same value. Thus, the two-parameter pseudo-component model does not adequately distinguish low MW cycloalkanes from low MW n-alkanes or PNAs. Decalin concentration may also play a role in higher deviations for viscosity predictions using the two-parameter model. However, decalin's effect is unclear as it was present in compositions of only mixture M1.

Another reason for deficiencies in the model could be due to the constant value of the *D* coefficient for every functional group in Lötgering-Lin and Gross [54]'s GC viscosity model. Extending their model to fit functional group dependent *D* coefficients could possibly lead to more accurate viscosity predictions without fitting *D* in the three-parameter model. It is also noted that

in the work of Lötgering-Lin and Gross, the pure component GC viscosity coefficients were fit using the homosegmented GC parameters of Sauer et al. [60], where iso and normal alkane functional groups were not differentiated when fitting parameters.

Nevertheless, the two-parameter model and the Z parameter from Eq. 5 do not appear to accurately represent mixtures containing significant concentrations of MCH and iso-alkanes. Inclusion of a single viscosity data point at a chosen reference state to fit the *D* coefficient offers the potential for improved viscosity predictions in the three-parameter model. Viscosity is predicted for hydrocarbon mixtures using the three-parameter model with an average MAPD of 7.3% for all compositions of all mixtures in this study. This result is comparable to the viscosity predictions of Gross and co-workers [55] (*i.e.*, 6.2% average MAPD) for non-polar binary mixtures.

Diesel Fuels

Diesel fuels contain hundreds of hydrocarbon compounds and vary in composition due to many factors, including crude oil composition, distillation conditions, and additional processing and blending required to meet quality specifications [80]. Table 6 lists the limited number of experimental studies reporting the viscosity of diesel fuels up to HTHP conditions. Detailed composition of diesel fuels, required for our analysis, was found only in Aquing et al. [13]. Although, Politte [81] provides limited fuel compositional information, their reported average CN and average MW were not found to be self-consistent. Therefore, the diesel fuel investigated by Politte [81] is not considered in this study. Further explanation for its exclusion is included in the SI. Aquing et al. [13] reported gas chromatography results of two diesel fuels (referred to in this study as Middle East SR and Highly Naphthenic) and measured the viscosity of these diesel fuels from 323 to 423 K and up to 3,500 bar. Table 7 lists the molar composition and CN range for different classes of compounds in the diesel fuels. Table 8 lists the number averaged MW, HN/CN

ratio, viscosity experimental data point (η_O) at the lowest reported temperature and pressure (*i.e.*, 323 K and ~10 bar) used to fit D in the three-parameter model, PC-SAFT parameters (Eqs. 2-4), and viscosity coefficients (Eqs. 12-15) of the pseudo-components for the two diesel fuels.

Table 6. Summary of viscosity data for diesel fuels measured up to high temperatures and pressures.

Author	Year	T_{range}/K	P_{max}/bar	Uncertainty (%)	No. of Samples with Composition
Schaschke et al. [12]	2013	298-373	5,000	2	0
Aquing et al. [13]	2012	323-423	3,500	2	2
Duncan et al. [82]	2012	283-373	1,311	-	0
Bazile et al. [83]	2012	293-353	2,000	1	0
Duncan et al. [84]	2010	283-373	1,311	-	0
Robertson and Schaschkle [85]	2009	273-294	1,600	-	0
Politte [81]	1985	298-422	1,000	-	1[a]

[a]Sample is not considered in this study. Explanation is provided in the SI.

Table 7. Molar composition (%) and carbon number ranges of chemical classes in diesel fuels measured by gas chromatography. Data from ref. [13].

	Mole Percent (%)		Carbon Number Range	
Chemical Class	Middle East SR	Highly Naphthenic	Middle East SR	Highly Naphthenic
n-alkanes	23	6	7-27	7-29
Iso-alkanes	26	13	7-27	7-29
Cyclohexanes	16	26	8-26	8-28
Decalins	4	20	10-25	10-26
Benzenes	10	10	8-24	8-20
Naphthalenes	7	3	10-21	10-15
Phenanthrenes	3	1	14-20	14-35
Tetralins and Indanes	7	16	9-23	9-22
Other unsaturates	4	5	12-21	13-35

Table 8. Pseudo-component properties and parameters for diesel fuels. η_O is the viscosity data point at the lowest reported temperature and pressure (*i.e.*, 323 K and ~10 bar) used to fit D, now termed D^{fit}, in the three-parameter model.

Diesel	MW	HN/CN	Z	η_O / cP	m	σ (Å)	ε/k (K)	A	B	C	D	D^{fit}
Middle East SR	225.1	1.85	0.222	2.97	7.202	3.846	254.6	-0.829	-3.885	-0.837	-0.203	-0.226
Highly Naphthenic	203.6	1.74	0.292	2.57	6.448	3.836	259.0	-0.780	-3.668	-0.771	-0.185	-0.211

Figures 5 and 6 show viscosity predictions and deviations from experiment, respectively, for the Middle East SR and Highly Naphthenic diesel fuels for three isotherms (323 K, 373 K, and 423 K) and pressures up to 3,500 bar. Viscosity is predicted across all conditions for both diesel fuels with an average MAPD of 22.0% using the two-parameter model and 9.3% using the three-parameter model. Table 9 presents the statistics for viscosity predictions of the diesel fuels. The composition of the diesel fuels in this study contain significant concentrations of iso-alkanes (*i.e.*, 26 mol% for the Middle East SR diesel fuel and 13 mol% for the Highly Naphthenic diesel fuel) and cyclohexanes (16 mol% and 26 mol% for the Middle East SR and Highly Naphthenic diesel fuels, respectively). Large concentrations of iso-alkanes and cyclohexanes in the diesel fuels are possibly the cause of less accurate predictions using the two-parameter model, similar to the compositions of mixtures M1 and M2. The Highly Naphthenic diesel fuel also contains 20 mol% decalins, which possibly is another cause of viscosity prediction deviations based on our observations for compositions of mixture M1. Inclusion of a single viscosity data point as a third parameter in the model improves viscosity predictions for the diesel fuels in this study.

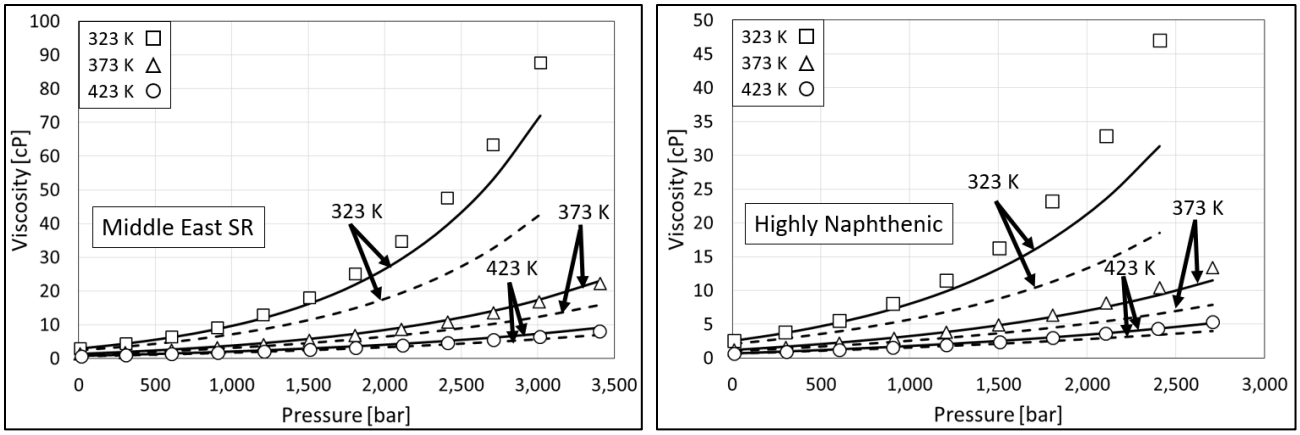

Figure 5. Pseudo-component viscosity predictions compared to experimental data [13] (symbols) for diesel fuels: two-parameter (dashed lines) and three-parameter (solid lines). Note that the y-axis scale is different in each figure.

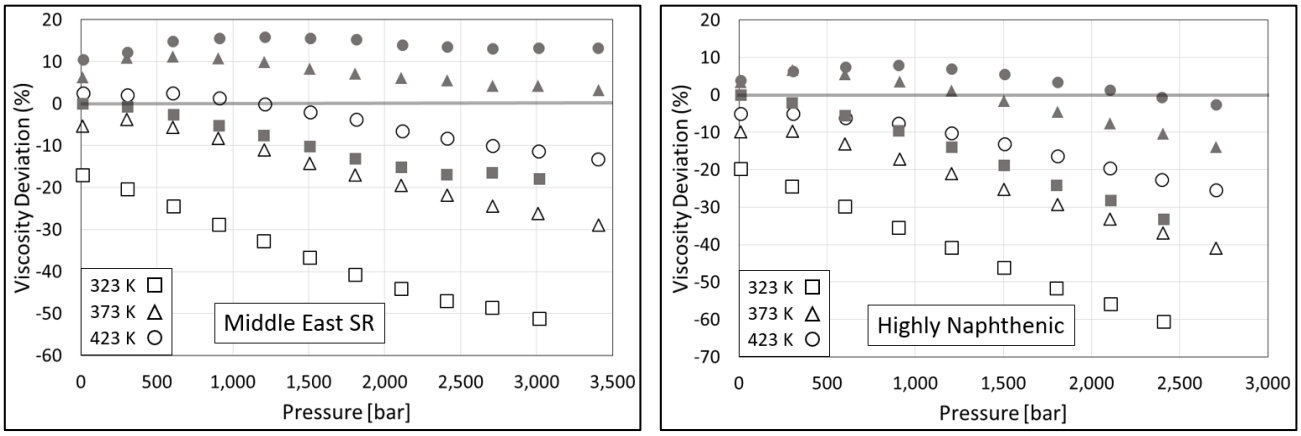

Figure 6. Pseudo-component viscosity deviations compared to experimental data [13] for diesel fuels: two-parameter (open symbols) and three-parameter (filled symbols) models. Note that the y-axis scale is different in each figure.

Table 9. The MAPD (%), bias (%), SD (%), and Max Deviation (%) for pseudo-component viscosity predictions of diesel fuels compared to experimental data [13].

	Two-parameter		Three-parameter	
	Middle East SR	Highly Naphthenic	Middle East SR	Highly Naphthenic
MAPD	18.3	25.2	10.3	8.3
Bias	-17.8	-25.2	4.3	-3.9
SD	15.2	15.7	5.0	8.3
Max Deviation	51.3	60.6	17.9	33.2

Conclusion

A pseudo-component technique based upon residual entropy scaling using the Perturbed-Chain Statistical Associating Fluid Theory was developed to predict the viscosity of hydrocarbon mixtures and diesel fuels. The model predicts viscosity without need to fit to high temperature and pressure experimental data and requires input of only two calculated or experimentally measured mixture properties: the number averaged molecular weight and hydrogen-to-carbon ratio. Inclusion of a third parameter, the viscosity data point at a chosen reference state was shown to improve predictions for mixtures that contained significant concentrations of iso-alkanes and cyclohexanes. The ability to predict accurate viscosities for complex hydrocarbon mixtures such as diesel fuel up to extreme conditions, using relatively simple inputs will aid the future development of fuel injection equipment design and support the development and optimization of fuel and fluid formulations for improved performance at extreme conditions.

Acknowledgments

This project has received funding from the European Union Horizon 2020 Research and Innovation program, Grant Agreement No 675528. The authors wish to thank Joseph Roos (Afton), Joseph Remias (Afton), Mark Devlin (Afton), Oliver Lötgering-Lin (University of Stuttgart), Joachim Gross (University of Stuttgart), and Rajendar Mallepally (Virginia Commonwealth University) for their helpful, technical discussions.

Nomenclature

English symbols

$\tilde{a}$	reduced Helmholtz free energy	N	number of data points
Å	Angstrom	N_A	Avogadro's number
A, B, C, and D	viscosity coefficients	$\bar{s}$	molar entropy
e	coefficient in the polynomial shown in Table 2		
CN	carbon number	$\tilde{s}$	reduced entropy
HN	hydrogen number	s^*	reduced dimensionless residual entropy
k	Boltzmann constant	T	temperature
K	Kelvin	V	volume
m	number of segments	Z	averaging parameter, Eq. 5

Greek symbols

σ	segment diameter	η	viscosity
$\Omega^{(2,2)*}$	reduced collision integral	η^*	reduced viscosity
ε/k	depth of the potential well	$\bar{\eta}$	viscosity mean
η_0	viscosity experimental data point at the lowest reported temperature and pressure		

Superscripts/Subscripts

CE	Chapman-Enskog	hc	hard-chain
disp	dispersion	predict	prediction
exp	experimental data	res	residual

References

[1] Zhao H. Advanced direct injection combustion engine technologies and development: diesel engines. Elsevier; 2009.

[2] Heywood JB. Fundamentals of internal combustion engines. Tata McGraw-Hill Education; 1988.

[3] European-Union. Effect of 4500bar injection pressure and super-critical phase change of surrogate and real-world fuels enriched with additives and powering Diesel engines on soot emissions reduction; 2015. Available from: https://cordis.europa.eu/project/rcn/198296_en.html. [Accessed 5 March 2018].

[4] Arcoumanis C, Gavaises, M. Linking nozzle flow with spray characteristics in a diesel fuel injection system. Atomization and Sprays **1998**;8(3):307-47.

[5] Battistoni M, Grimaldi, C.N. Numerical analysis of injector flow and spray characteristics from diesel injectors using fossil and biodiesel fuels. Applied Energy **2012**;97:656-66.

[6] Giannadakis E, Gavaises, M., Arcoumanis, C. . Modelling of cavitation in diesel injector nozzles. Journal of Fluid Mechanics **2008**;616:153-93.

[7] Park SH, Suh, H.K., Lee, C.S. Effect of cavitating flow on the flow and fuel atomization characteristics of biodiesel and diesel fuels. Energy & Fuels **2007**;22(1):605-13.

[8] Pomraning E, Richards, K., Senecal, P.K.,. Modeling turbulent combustion using a RANS model, detailed chemistry, and adaptive mesh refinement. SAE Technical Paper **2014**;2014-01-1116.

[9] Schmidt DP, Corradini, M.L. The internal flow of diesel fuel injector nozzles: A review. International Journal of Engine Research **2001**;2(1):1-22.

[10] Senecal PK, Pomraning, E., Richards, K., Som, S. Grid convergent spray models for internal combustion engine CFD simulations. ASME 2012 Internal Combustion Engine Division Fall Technical Conference **2012**:697-710.

[11] Theodorakakos A, Strotos, G., Mitroglou, N., Atkin, C., Gavaises, M.,. Friction-induced heating in nozzle hole micro-channels under extreme fuel pressurisation. Fuel 2014;123:143-50.
[12] Schaschke C, Fletcher, I., Glen, N.,. Density and viscosity measurement of diesel fuels at combined high pressure and elevated temperature. Processes 2013;1(2):30-48.
[13] Aquing M, Ciotta, F., Creton, B., Féjean, C., Pina, A., Dartiguelongue, C., Trusler, J.P.M., Vignais, R., Lugo, R., Ungerer, P. Composition analysis and viscosity prediction of complex fuel mixtures using a molecular-based approach. Energy & Fuels 2012;26(4):2220-30.
[14] Baled HO, Gamwo, I.K., Enick, R.M., M°Hugh, M.A. Viscosity models for pure hydrocarbons at extreme conditions: A review and comparative study. Fuel 2018;218:89-111.
[15] Alade OS, Ademodi, B., Sasaki, K., Sugai, Y., Kumasaka, J., Ogunlaja, A.S. Development of models to predict the viscosity of a compressed Nigerian bitumen and rheological property of its emulsions. Journal of Petroleum Science and Engineering 2016;145:711-22.
[16] Eghbali S, Dehghanpour, H., Dragani, J., Zhang, X., . Phase Behaviour and Viscosity of Bitumen-CO 2/Light Hydrocarbon Mixtures at Elevated Temperatures: A Cold Lake Case Study. *SPE Canada Heavy Oil Technical Conference.* Calgary, Alberta, Canada: Society of Petroleum Engineers; 2018.
[17] Gülüm M, Bilgin, A. Measurements and empirical correlations in predicting biodiesel-diesel blends' viscosity and density. Fuel 2017;199(567-77).
[18] Bair S. The pressure and temperature dependence of volume and viscosity of four Diesel fuels. Fuel 2014;135:112-9.
[19] Ilyin SO, Strelets, L.A. Basic Fundamentals of Petroleum Rheology and Their Application for the Investigation of Crude Oils of Different Natures. Energy & Fuels 2018;32(1):268-78.
[20] Kanaveli IP, Atzemi, M., Lois, E. Predicting the viscosity of diesel/biodiesel blends. Fuel 2017;199:248-63.
[21] Lapuerta M, Rodríguez-Fernández, J., Fernández-Rodríguez, D., Patiño-Camino, R. Modeling viscosity of butanol and ethanol blends with diesel and biodiesel fuels. Fuel 2017;199:332-8.
[22] Rodriguez C, Vidal, A., Koukouvinis, P., Gavaises, M., M°Hugh, M.A.,. Simulation of transcritical fluid jets using the PC-SAFT EoS. Journal of Computational Physics (In Press) 2018.
[23] Parsa A, Srinivasan, S., Saghir, M.Z. Impact of density gradients on the fluid flow inside a vibrating cavity subjected to soret effect. The Canadian Journal of Chemical Engineering 2013;91(3):550-9.
[24] Rodriguez C, Vidal, A., Koukouvinis, P., Gavaises, M.,. Supercritical and transcritical real-fluid mixing using the PC-SAFT EOS. *Ilass Europe, 28th Conference on Liquid Atomization and Spray Systems.* Valencia, Spain; 2017:597-64.
[25] Burgess WA, Bamgbade, B.A., Gamwo, I.K. Experimental and predictive PC-SAFT modeling results for density and isothermal compressibility for two crude oil samples at elevated temperatures and pressures. Fuel 2018;218:385-95.
[26] Aminian A, ZareNezhad, B. Accurate predicting the viscosity of biodiesels and blends using soft computing models. Renewable Energy 2018;120:488-800.

[27] Grandelli HE, Dickmann, J.S., Devlin, M.T., Hassler, J.C., Kiran, E. Volumetric properties and internal pressure of poly (α-olefin) base oils. Industrial & Engineering Chemistry Research 2013;52(50):17725-34.
[28] Tran TC, Logan, G.A., Grosjean, E., Harynuk, J., Ryan, D., Marriott, P.,. Comparison of column phase configurations for comprehensive two dimensional gas chromatographic analysis of crude oil and bitumen. Organic Geochemistry 2006;37(9):1190-4.
[29] Nishioka M, Bradshaw, J.S., Lee, M.L., Tominaga, Y., Tedjamulia, M., Castle, R.N. Capillary column gas chromatography of sulfur heterocycles in heavy oils and tars using a biphenyl polysiloxane stationary phase. Analytical Chemistry 1985;57(1):309-12.
[30] Mueller CJ, Cannella, W.J., Bays, J.T., Bruno, T.J., DeFabio, K., Dettman, H.D., Gieleciak, R.M., Huber, M.L., Kweon, C.B., M^{c}Connell, S.S., Pitz, W.J. . Diesel surrogate fuels for engine testing and chemical-kinetic modeling: Compositions and properties. Energy & Fuels 2016;30(2):1445-61.
[31] Mueller CJ, Cannella, W.J., Bruno, T.J., Bunting, B., Dettman, H.D., Franz, J.A., Huber, M.L., Natarajan, M., Pitz, W.J., Ratcliff, M.A., Wright, K. Methodology for formulating diesel surrogate fuels with accurate compositional, ignition-quality, and volatility characteristics. Energy & Fuels 2012;26(6):3284-303.
[32] Anand K, Ra, Y., Reitz, R. D., Bunting, B. Surrogate model development for fuels for advanced combustion engines. Energy & Fuels 2011;25(4):1474-84.
[33] Herbinet O, Pitz, W.J., Westbrook, C.K. Detailed chemical kinetic mechanism for the oxidation of biodiesel fuels blend surrogate. Combustion and Flame 2010;157(5):893-908.
[34] Huber ML, Lemmon, E.W., Diky, V., Smith, B.L., Bruno, T.J. . Chemically authentic surrogate mixture model for the thermophysical properties of a coal-derived liquid fuel. Energy & Fuels 2008;22(5):3249-57.
[35] Pitz WJ, Mueller, C.J. Recent progress in the development of diesel surrogate fuels. Progress in Energy and Combustion Science 2011;37(3):330-50.
[36] Lin R, Tavlarides, L.L. Thermophysical properties needed for the development of the supercritical diesel combustion technology: Evaluation of diesel fuel surrogate models. The Journal of Supercritical Fluids 2012;71:136-46.
[37] Yarranton HW, Satyro, M.A.,. Expanded fluid-based viscosity correlation for hydrocarbons. Industrial & Engineering Chemistry Research 2009;48(7):3640-8.
[38] Motahhari H, Satyro, M.A., Taylor, S.D., Yarranton, H.W. Extension of the expanded fluid viscosity model to characterized oils. Energy & Fuels 2013;27(4):1881-98.
[39] Motahhari H, Schoeggl, F., Satyro, M., Yarranton, H. Viscosity prediction for solvent-diluted live bitumen and heavy oil at temperatures up to 175-deg-C. Journal of Canadian Petroleum Technology 2013;52(5):376-90.
[40] Ma M, Chen, S., Abedi, J. Modeling the density, solubility and viscosity of bitumen/solvent systems using PC-SAFT. Journal of Petroleum Science and Engineering 2016;139:1-12.
[41] Quiñones-Cisneros SE, Zéberg-Mikkelsen, C.K., Stenby, E.H.,. The friction theory (f-theory) for viscosity modeling. Fluid Phase Equilibria 2000;169(2):249-76.
[42] Quiñones-Cisneros SE, Zéberg-Mikkelsen, C.K., Baylaucq, A., Boned, C.,. Viscosity modeling and prediction of reservoir fluids: From natural gas to heavy oils. International journal of thermophysics 2004;25(5):1353-66.
[43] Quiñones-Cisneros SE, Dalberg, A., Stenby, E.H.,. PVT characterization and viscosity modeling and prediction of crude oils. Petroleum science and technology 2004;22((9-10)):1309-25.

[44] Schmidt KA, Quiñones-Cisneros, S.E., Kvamme, B.,. Density and viscosity behavior of a North Sea crude oil, natural gas liquid, and their mixtures. Energy & fuels 2005;19(4):1303-13.
[45] Abutaqiya MI, Zhang, J., Vargas, F.M. Viscosity modeling of reservoir fluids using the Friction Theory with PC-SAFT crude oil characterization. Fuel 2019;235:113-29.
[46] Khoshnamvand Y, Assareh, M. Viscosity Prediction for Petroleum Fluids Using Free Volume Theory and PC-SAFT. International Journal of Thermophysics 2018;39(4):54.
[47] Sun Y, Shen, G., Held, C., Lu, X., Ji, X.,. Modeling Viscosity of Ionic Liquids with Electrolyte Perturbed-Chain Statistical Associating Fluid Theory and Free Volume Theory. Industrial & Engineering Chemistry Research 2018;57(26):8784-801.
[48] Assael MJ, Dymond, J.H., Tselekidou, V. Correlation of high-pressure thermal conductivity, viscosity, and diffusion coefficients for n-alkanes. International journal of thermophysics 1990;11(5):863-73.
[49] Dymond JH, Awan, M.A. Correlation of high-pressure diffusion and viscosity coefficients for n-alkanes. International journal of Thermophysics 1989;10(5):941-51.
[50] Ijaz F. Measurement and Prediction of the Viscosity of Hydrocarbon Mixtures and Crude Oils. Imperial College, London; 2011.
[51] Macias-Salinas R, Durán-Valencia, C., López-Ramírez, S., Bouchot, C. Eyring-theory-based model to estimate crude oil viscosity at reservoir conditions. Energy & Fuels 2008;23(1):464-70.
[52] Eyring H. Viscosity, plasticity, and diffusion as examples of absolute reaction rates. The Journal of chemical physics 1936;4(4):283-91.
[53] Rosenfeld Y. Relation between the transport coefficients and the internal entropy of simple systems. Physical Review A **1977**;15(6).
[54] Lötgering-Lin O, Gross, J. Group contribution method for viscosities based on entropy scaling using the perturbed-chain polar statistical associating fluid theory. Industrial & Engineering Chemistry Research **2015**;54(32):7942-52.
[55] Lötgering-Lin O, Fischer, M., Hopp, M., Gross, J. Pure Substance and Mixture Viscosities Based on Entropy Scaling and an Analytic Equation of State. Industrial & Engineering Chemistry Research 2018;57(11):4095-114.
[56] Fouad WA, Vega, L.F. On the anomalous composition dependence of viscosity and surface tension in refrigerant blends. Journal of Molecular Liquids 2018;268:190-200.
[57] Fouad WA, Vega, L.F. Transport properties of HFC and HFO based refrigerants using an excess entropy scaling approach. The Journal of Supercritical Fluids 2018;131:106-16.
[58] Rokni HB, Gupta, A., Moore, J.D., M^{c}Hugh, M.A., Bamgbade, B.A., Gavaises, M. Purely predictive method for density, compressibility, and expansivity for hydrocarbon mixtures and diesel and jet fuels up to high temperatures and pressures. Fuel **2019**;236:1377-90.
[59] Gross J, Sadowski, G. Perturbed-chain SAFT: An equation of state based on a perturbation theory for chain molecules. Industrial & engineering chemistry research **2001**;40(4):1244-60.
[60] Sauer E, Stavrou, M., Gross, J. Comparison between a homo-and a heterosegmented group contribution approach based on the perturbed-chain polar statistical associating fluid theory equation of state. Industrial & Engineering Chemistry Research **2014**;53(38):14854-64.
[61] Laursen T. VLXE, V. 9.3 www.vlxe.com. **2017**.
[62] Novak L. Self-diffusion coefficient and viscosity in fluids. Journal of Chemical Reactor Engineering 2011;9(1).

[63] Novak L. Fluid viscosity-residual entropy correlation. International Journal of Chemical Reactor Engineering 2011;9(1).
[64] Neufeld PD, Janzen, A.R., Aziz, R.A. Empirical equations to calculate 16 of the transport collision integrals Ω (l, s)* for the Lennard-Jones (12–6) potential. The Journal of Chemical Physics 1972;57(3):1100-2.
[65] International A. ASTM D445-12 Standard Test Method for Kinematic Viscosity of Transparent and Opaque Liquids (and Calculation of Dynamic Viscosity). West Conshohocken, PA; 2012.
[66] Zéberg-Mikkelsen CK, Barrouhou, M., Baylaucq, A., Boned, C. High-pressure viscosity and density measurements of the ternary system methylcyclohexane+ cis-decalin+ 2, 2, 4, 4, 6, 8, 8-heptamethylnonane. Journal of Chemical & Engineering Data 2003;48(6):1387-92.
[67] Baylaucq A DP, Boned C. Viscosity and density of the ternary mixture heptane+ methylcyclohexane+ 1-methylnaphthalene. International journal of thermophysics 1997;18(5):1089-107.
[68] Boned C, Zéberg-Mikkelsen, C.K., Baylaucq, A., Daugé, P. High-pressure dynamic viscosity and density of two synthetic hydrocarbon mixtures representative of some heavy petroleum distillation cuts. Fluid phase equilibria 2003;212(1):143-64.
[69] Dauge P, Canet, X., Baylaucq, A., Boned, C. Measurements of the density and viscosity of the tridecane+ 2, 2, 4, 4, 6, 8, 8-heptamethylnonane mixtures in the temperature range 293.15-353.15 K at pressures up to 100 MPa. High Temerpatures High Pressures 2001;33(2):213-30.
[70] Zeberg-Mikkelsen CK, Canet, X., Baylaucq, A., Quiñones-Cisneros, S.E., Boned, C., Stenby, E.H. High-pressure viscosity and density behavior of ternary mixtures: 1-methylnaphthalene+ n-tridecane+ 2, 2, 4, 4, 6, 8, 8-heptamethylnonane. International journal of thermophysics 2001;22(6):1691-726.
[71] Baylaucq A, Zeberg-Mikkelsen, C.K., Daugé, P., Boned, C. Dynamic viscosity and density of heptylbenzene and heptylcyclohexane up to 100 MPa. Journal of Chemical & Engineering Data 2002;47(4):997-1002.
[72] Caudwell DR, Trusler, J.M., Vesovic, V., Wakeham, W.A. Viscosity and Density of Five Hydrocarbon Liquids at Pressures up to 200 MPa and Temperatures up to 473 K. Journal of Chemical & Engineering Data 2008;54(2):359-66.
[73] Haynes WM. CRC handbook of chemistry and physics. CRC press; 2014.
[74] Michailidou EK, Assael, M.J., Huber, M.L., Abdulagatov, I.M., Perkins, R.A. Reference Correlation of the Viscosity of n-Heptane from the Triple Point to 600 K and up to 248 MPa. Journal of Physical and Chemical Reference Data 2014;43(2):1-13.
[75] Oshmyansky Y, Hanley, H.J.M., Ely, J.F., Kidnay, A.J. The viscosities and densities of selected organic compounds and mixtures of interest in coal liquefaction studies. International Journal of Thermophysics 1986;7(3):599-608.
[76] Pereiro AB, Rodríguez, A., Canosa, J., Tojo, J. Density, viscosity, and speed of sound of dialkyl carbonates with cyclopentane and methyl cyclohexane at several temperatures. Journal of Chemical & Engineering Data 2004;49(5):1392-9.
[77] Rafiee HR, Ranjbar, S., Poursalman, F. Densities and viscosities of binary and ternary mixtures of cyclohexanone, 1, 4-dioxane and isooctane from T=(288.15 to 313.15) K. The Journal of Chemical Thermodynamics 2012;54:266-71.

[78] Van Velzen D, Lopes Cardozo, R., Langenkamp, H. Liquid Viscosity and Chemical Constitution of Organic Compounds: A New Correlation and a Compilation of Literature Data. Joint Nuclear Research Centre - Ispra Establishment (Italy): Commission of the European Communities; 1972.
[79] Krahn UG, Luft, G. Viscosity of several liquid hydrocarbons in the temperature range 298-453 K at pressures up to 200 MPa. Journal of Chemical and Engineering Data 1994;39(4):670-2.
[80] ASTM International. ASTM D975-18 Standard Specification for Diesel Fuel Oils. West Conshohocken, PA; **2018**.
[81] Politte MD. Invert oil mud rheology as a function of temperature and pressure. *SPE/IADC Drilling Conference* Society of Petroleum Engineers.; 1985.
[82] Duncan AM, Pavlicek, N., Depcik, C.D., Scurto, A.M., Stagg-Williams, S.M. High-pressure viscosity of soybean-oil-based biodiesel blends with ultra-low-sulfur diesel fuel. Energy & Fuels 2012;26(11):7023-36.
[83] Bazile JP, Nasri, D., Boned, C., Daridon, J.L. High pressure thermophysical characterization of fuel used for testing and calibrating diesel injection systems. Fuel 2012;98:288-94.
[84] Duncan AM, Ahosseini, A., M^{c}Henry, R., Depcik, C.D., Stagg-Williams, S.M., Scurto, A.M. High-pressure viscosity of biodiesel from soybean, canola, and coconut oils. Energy & Fuels 2010;24(10):5708-16.
[85] Robertson LX, Schaschke, C.J.,. Combined high pressure and low temperature viscosity measurement of biodiesel. Energy & Fuels 2009;24(2):1293-7.